

Interpretable-by-Design Transformers via Architectural Stream Independence

Clayton Kerce *

Georgia Tech Research Institute

clayton.kerce@gtri.gatech.edu and

Alexis Fox

Georgia Tech Research Institute

alexis.fox@duke.edu

Abstract

While transformers achieve strong performance, their internal decision-making processes remain opaque. We investigate whether architectural constraints can enforce *interpretability by design* through **architectural stream independence**: maintaining a **token stream** (carrying symbolic structure) and **contextual semantics** in separated streams that remain independently observable throughout processing, with integration delayed until output.

We validate this principle through the Late Fusion Architecture (LFA), which demonstrates **interpretable symbolic heads through all the final layers**, while standard transformers show dissolution by the third of six layers; we quantify this effect by introducing the Token-Position Dependence Score (PDS), with $PDS_{max} = 0.276$ and 0.058 , respectively. Crucially, intervention experiments demonstrate functional modularity: suppressing LFA’s recency heads causes minimal semantic damage (Cohen’s $d = -0.158$) versus catastrophic entanglement in baselines ($d = -0.672$).

LFA demonstrates that architectural constraints improve underlying learning mechanisms, averaging 42% stability versus 19% and 11% for baseline comparisons, with extremes from 50% on LFA’s best pairs (6 of 12 heads position-invariant) down to 0% complete collapse in over-constrained cases. By preventing premature entanglement, architectural independence steers models toward semantic understanding over positional heuristics, establishing interpretability as an architectural design criterion enforceable through structural constraints rather than post-hoc analysis.

1 Introduction

Despite the success of transformer-based language models, their internal mechanisms remain largely opaque. When models exhibit failures, e.g. recency bias (Guo and Vosoughi, 2025), sycophancy (Sharma et al., 2024), or spurious correlations (Yang et al., 2024), practitioners lack tools for understanding and addressing root causes. Post-hoc interpretability methods (Belinkov et al., 2017; Clark et al., 2019) reveal what models learn or where they attend, but do not provide paths toward models that are interpretable *by design*.

It is natural to ask: *Can we identify specific mechanisms within a model’s internal activations that control high-level behaviors?* This work directly addresses a strong form of explainability: rather than analyzing what emerged during training, can we design architectures that are more interpretable by construction? We answer affirmatively by demonstrating that **architectural constraints can promote transparent reasoning pathways** whose internal mechanisms are modular and independently observable.

To this end, we test a specific architectural hypothesis: **architectural stream independence**—maintaining a *token stream* and *contextual semantics* in separated streams that remain independently observable throughout processing—preserves functional modularity, creating models whose mechanisms can be directly observed and independently intervened upon. This contrasts with immediate integration architectures that immediately mix symbolic structure and contextual information, causing symbolic structure signals to dissolve into entangled representations.

This design is motivated by intuitions about distinct computational roles—symbolic routing via attention, pattern discovery through circuit formation, and contextual elaboration via the feed-forward network (Appendix B)—that benefit from

*This work was partially supported by contract HR001125C0302

architectural separation. We implement architectural stream independence through **asymmetric information flow**: a frozen position stream (X_T , carrying symbolic structure) influences contextual updates (X_E) without being corrupted by gradient flow, with symmetric combination only at the output layer (lm_head). Unlike DeBERTa’s additive decomposition within attention (He et al., 2021), our approach maintains independent observability: symbolic structure remains a clean, surgically analyzable signal throughout all transformer layers.

Notation. We distinguish between the **absolute token index** $i \in \{0, \dots, T - 1\}$ and the **relative token position** $p = i_{\text{target}} - i$ (used in intervention analysis). We denote *layer index* by ℓ and *head index* by h . The model maintains two parallel streams: a frozen token stream X_T encoding symbolic structure, and a mutable contextual stream X_E .

We validate this through the Late Fusion Architecture (LFA), demonstrating: (1) functional transparency as a design criterion with quantitative metrics; (2) systematic comparison of four architectural variants isolating constraint effects; and (3) empirical validation showing LFA maintains interpretable position channels in layers 4-5 ($\text{PDS}_{\text{max}} = 0.276$) where immediate integration architectures show premature dissolution ($\text{PDS}_{\text{max}} = 0.058$), with measurably lower intervention collateral damage (Cohen’s $d = -0.158$ vs. -0.672 for entangled baselines).

Our coreference experiments show that LFA’s specialists concentrate in mid-to-late layers (top head L4.H3: 48.3%), while standard transformers’ best heads are distributed across layers (best head L1.H5: 46.9%; Table 3). We validate using small models (13M-22M parameters) on TinyStories, providing clean evidence that **interpretability can be designed into architectures through principled constraints**, offering a path toward transparent, explainable language models where internal reasoning processes can be directly observed and understood.

2 Architecture and Design Principles

2.1 Architectural Stream Independence: The Design Principle

We define **architectural stream independence** as maintaining a token stream and **contextual semantics** in separated streams that remain indepen-

dently observable throughout transformer processing, with integration occurring only at the output layer. This design principle creates transparent reasoning pathways where distinct mechanisms can be directly observed and independently intervened upon.

Standard transformers violate this principle through **immediate integration**: token position encodings and token identities are added at layer 0 and immediately mixed with semantic features via dense attention. By layer 2, symbolic structure dissolves into distributed semantic representations, making it impossible to isolate which heads track **symbolic identities** versus meaning (Figure 1, Std-T panel).

The Late Fusion Architecture (LFA) implements architectural stream independence through delayed integration: *token stream* and *contextual semantics* remain separated until output-layer combination. This “late fusion” timing preserves functional modularity—by keeping streams independent until the model has developed rich semantic representations, we create mechanisms that remain independently observable and interventionable.

This design generates four testable predictions:

1. **Preserved observability:** LFA maintains independently observable **symbolic heads** in deep layers (L4-L5), validated by high PDS
2. **Early dissolution:** Immediate integration architectures show symbolic structure dissolving by layer 2, validated by low PDS
3. **Functional independence:** Separated streams enable surgical interventions on **recency heads** without semantic damage
4. **Entangled opacity:** Immediate integration creates inseparable mechanisms where interventions cause catastrophic collateral damage

2.2 Stream Separation Mechanism

We implement architectural stream independence through **separation of streams**. The model maintains:

- **Frozen token stream** (X_T): preserves symbolic structure and token position unchanged
- **Embedding stream** (X_E): accumulates semantic updates

Formally:

$$\begin{aligned} X_T^{(0)} &= \text{TokenEmbedding}(\text{input}), \quad X_E^{(0)} = 0 \\ X_T^{(\ell)} &= X_T^{(0)} \quad (\text{frozen across all layers}) \end{aligned} \quad (1)$$

The embedding stream updates via:

$$\begin{aligned} X_E^{(\ell)} &= X_E^{(\ell-1)} + \text{Attn}(Q, K, X_T^{(0)}) \\ &\quad + \text{FFN}(X_T + X_E) \end{aligned} \quad (2)$$

Critically, while the FFN incorporates positional information into semantic processing (observing $X_T + X_E$), it maintains architectural separation by writing only to X_E . This **asymmetric information flow** allows token position and symbolic structure to inform semantic learning while preserving the token stream as a clean, independently observable signal. Attention similarly reads from both streams but writes only to X_E .

The streams remain separated until `lm_head` combines them for final prediction:

$$\text{logits} = \text{LM_head}(\text{LayerNorm}(X_T + X_E)) \quad (3)$$

This delayed **symmetric combination** is the “late” in late fusion—symbolic structure remains independently observable throughout all internal processing, with no gradient flow corrupting X_T .

2.3 Distinction from Prior Disentanglement

DeBERTa computes separate position-content attention terms but allows immediate mixing (He et al., 2021). Our frozen stream enforces **architectural separation** with no gradient flow between streams. DeBERTa disentangles *how* attention is computed; we control *where* updates are written. This architectural constraint, combined with independent channels (ChannelLayerNorm + Kronecker mixing), maintains complete separation throughout all transformer layers until the final output.

2.4 Why Asymmetric Flow Maintains Architectural Independence

The asymmetric information flow ($X_T \rightarrow X_E$, but X_T frozen) is critical for maintaining architectural stream independence:

1. **Position never corrupted:** X_T receives no gradient updates, remaining a clean position signal

Property	Immediate Integration (Std-T)	Stream Independence (LFA)
Position encoding	Added at L0	Frozen in X_T
Stream separation	None	X_T / X_E distinct
Information flow	Bidirectional	$X_T \rightarrow X_E$ only
Position observable L5	No (PDS=0.058)	Yes (PDS=0.276)
Integration timing	Every layer	lm_head only
Gradient flow to X_T	Yes	No

Table 1: **Immediate integration vs. architectural stream independence.** LFA maintains independent observability through asymmetric information flow and delayed symmetric combination.

2. **Semantics benefit from position:** FFN observes $X_T + X_E$, enabling position-aware semantic processing
3. **Independent observability preserved:** Both streams remain surgically analyzable and interventionable
4. **Delayed integration:** Symmetric combination (`lm_head`) occurs between independently-evolved, mature representations

High PDS in deep layers validates that architectural independence is maintained: position signals remain distinct and independently observable. If premature integration occurred (as in standard transformers), position would dissolve into distributed semantic representations, destroying independent observability.

Table 1 summarizes the architectural contrast between early and late fusion.

2.5 Architectural Constraints

Frozen Token Stream (FTS): Token embeddings initialize $X_T^{(0)}$, while $X_E^{(0)} = 0$. In FTS, attention reads from the frozen token stream and writes to the embedding stream; X_T is held fixed across layers while all parameters train end-to-end. Channelization is preserved by construction (identity W_V and W_O in FTS). Complete stream separation is maintained throughout all transformer layers; fusion occurs only at the output layer (`lm_head`). See Appendix A for the formal update rules.

2.6 Model Configurations

We train four models to test our hypothesis and ablate architectural components (Table 2):

Model	Attn	FFN	Params	Val Loss
Std-T	dns	dns	22.2M	1.8114
D-Cas	dns	dns	21.2M	1.8399
LFA	ind	dns	18.5M	1.9063
CFM	ind	ind	13.4M	2.1019

Table 2: Model configurations and training performance. All models have 6 layers, 6 heads, 384d embeddings, trained on 2M samples from TinyStories for 2 epochs.

LFA (Late Fusion Architecture): Implements architectural stream independence via FTS + independent attention + dense FFN. Maintains separated streams with integration delayed until output.

Std-T (Standard Transformer): Single-stream with dense attention and FFN (GPT-2 style). Immediate integration baseline.

D-Cas (Dense Attention Baseline): FTS + dense attention + dense FFN. Tests whether frozen stream alone improves interpretability.

CFM (Channel-Factored Model): FTS + independent attention + independent FFN. Tests whether excessive constraint degrades learning.

All models use 6 layers, 6 heads, trained on TinyStories for 2 epochs. Model sizes vary by constraint (13.4M-22.2M parameters). The dense FFN in LFA serves a dual computational role: (1) it observes both streams to inform semantic updates, enabling rich contextual processing while (2) writing only to X_E , maintaining architectural separation. Unlike CFM’s independent FFN which cannot coordinate across heads, LFA’s dense FFN enables semantic coordination while preserving channel independence in attention. Critically, fusion occurs only at lm_head , combining the frozen token stream (X_T) with matured semantic representations (X_E). While our experiments focus on validating the interpretability benefits of architectural separation, the computational motivations behind these design choices are discussed in Appendix B.

3 Explainability Methodology: Isolating Positional from Semantic Reasoning

3.1 Coreference Resolution Analysis

We construct a ground truth dataset of 29 coreference instances across 13 diagnostic prompts, each specifying a pronoun (query token) and correct antecedent. The dataset includes minimal pairs testing specific phenomena: competing nouns (se-

mantic appropriateness vs. positional recency), gender resolution, and plurality agreement. For example, competing noun pairs test whether models attend to semantically appropriate targets regardless of position: “Tim saw a *key* and a box. He used it” vs. “Tim saw a box and a *key*. He used it.”

Example behavior: Consider the minimal pair testing semantic appropriateness versus positional recency. For “Tim saw a box and a key. He used it” (key first), LFA’s top coreference head (L4.H3) attends to “key” with weight 0.303. When positions reverse (“Tim saw a key and a box. He used it”, key last), the same head increases attention to “key” (0.409), demonstrating **token position-invariant** semantic tracking—it identifies the semantically appropriate tool regardless of position.

Std-T lacks such specialization. Its best performing head (L3.H2) shows weaker attention to the correct antecedent in both positions (0.226 and 0.324), and the stability metric for this minimal pair shows the architectural difference: LFA has 0.50 stability (6 stable heads across the pair), while Std-T has 0.25 stability (1 stable head). CFM’s 0% stability (no consistent heads) reveals complete failure to develop semantic specialists, demonstrating pure recency bias.

We define three metrics quantifying attention patterns. **Mean Attention Weight** measures average attention mass from query to correct antecedent:

$$\text{Attn}_{\text{mean}} = \frac{1}{N} \sum_{i=1}^N \alpha_{q \rightarrow t}^{(i)} \quad (4)$$

Top1 Accuracy is the percentage where the correct antecedent receives highest attention:

$$\text{Top1} = \frac{|\{i : \arg \max_j \alpha_{q \rightarrow j}^{(i)} = t\}|}{N} \times 100\% \quad (5)$$

Stability measures consistent target preference across position variations:

$$\text{Stability} = \frac{|\{\text{heads} : \text{target}_{\text{first}} = \text{target}_{\text{last}}\}|}{|\text{total heads}|} \times 100\% \quad (6)$$

See Appendix J for complete dataset specification and examples.

3.2 Token-Position Dependence Score

To measure whether architectural separation successfully preserves symbolic structure and token

position as an independently observable signal, we introduce the Token-Position Dependence Score (PDS). High PDS indicates position remains distinct (maintained stream independence); low PDS indicates position has dissolved into semantic representations (premature integration). The delayed integration timing in LFA refers to *when symbolic structure ceases to be independently observable*: LFA maintains observability throughout all layers, integrating only at output.

For each head and minimal pair (target first vs. last):

$$\text{PDS}_{(\ell,h)} = \left| \frac{1}{K} \sum_{k=1}^K \alpha_{q \rightarrow t_{\text{last}}}^{(k)} - \frac{1}{K} \sum_{k=1}^K \alpha_{q \rightarrow t_{\text{first}}}^{(k)} \right| \quad (7)$$

where $K = 29$ minimal pairs. We use threshold $\text{PDS} > 0.075$ ($\mu + \sigma$ for Std-T) for descriptive counts, but interventions use ranked top- k selection. See Appendix C for threshold justification and full distributions.

3.3 Measuring Functional Transparency via Intervention

To validate that **positional** mechanisms are functionally independent from semantic processing, we perform targeted lesion studies using *relative token position* (p). For each model, we rank heads by PDS, select top- k *recency heads* ($k \in \{1, 2, 3, 5\}$), and apply soft gating to outputs ($g \in \{1.0, 0.75, 0.5, 0.25, 0.0\}$). We measure impact using Semantic Preference Score (SPS) on 60 competing-noun prompts:

$$\text{SPS} = \frac{1}{M} \sum_{m=1}^M \left(\alpha_{q \rightarrow \text{semantic}}^{(m)} - \alpha_{q \rightarrow \text{distractor}}^{(m)} \right) \quad (8)$$

where $M = 58$ (after filtering), semantic = tool, distractor = container.

We quantify functional independence using Cohen’s d effect size (Eq. 9), where small $|d|$ near zero indicates transparent functional decomposition. We include matched-random suppression, semantic suppression (bottom- k PDS), and baseline controls. See Appendix D for complete gating protocol, soft-suppression curves, and per-category analyses.

$$d = \frac{\mu_{\text{intervention}} - \mu_{\text{baseline}}}{\sigma_{\text{pooled}}} \quad (9)$$

4 Transparent Functional Decomposition

Architectural stream independence preserves functional modularity by preventing immediate

Head	Mean Attn		Top1 Acc	
	LFA	Std-T	LFA	Std-T
L4.H3	0.323	0.033	48.3%	6.9%
L3.H5	0.265	0.047	48.3%	6.9%
L4.H0	0.211	0.045	44.1%	13.1%
L4.H1	0.286	0.060	37.2%	13.1%
L3.H0	0.225	0.049	46.9%	4.8%

Table 3: **Coreference specialization: LFA vs. Std-T.** LFA’s top 5 coreference heads (ranked by mean attention) compared to the same head positions in Std-T. LFA concentrates specialists in L3-L4; these same positions in Std-T show weak, diffuse patterns. Std-T’s actual best heads (L1.H5: 46.9%, L3.H2: 44.8%) are distributed across different layers, requiring search to locate.

entanglement of *symbolic structure* and *context*. We test this via coreference resolution, which requires entity tracking across token positions without positional confounds. **Predictions:** (1) LFA shows concentrated specialization (few strong heads), (2) Std-T shows diffuse patterns (many weak heads), (3) heads are **token position-invariant**. Section 5.1 validates prediction (1), Section 4.2 validates (3).

4.1 Coreference Head Specialization

LFA exhibits strong head specialization concentrated in identifiable locations. The top head (L4.H3) correctly resolves 48.3% of all instances with mean attention 0.323; co-primary head L3.H5 achieves identical coverage (48.3%) with mean 0.265. These heads concentrate in mid-to-late layers (L3-L4), forming a coherent, easily identifiable processing module.

Std-T develops specialists with comparable peak performance (best head L1.H5: 46.9%), but distributes them diffusely across layers. Table 3 compares LFA’s top coreference heads to the same head positions in Std-T, revealing the architectural difference: LFA’s concentration in L3-L4 versus Std-T’s distribution across L1, L3, and other layers. This concentration enables direct observation—when analyzing coreference in LFA, one examines L4.H3; in Std-T, specialists must be located through search across all 36 heads. LFA’s top 5 heads all exceed 37% Top1 accuracy; those same head positions in Std-T show weak, inconsistent patterns, with most below 15% (see Appendix E for complete results across all 36 heads).

4.2 Token-Position-Invariant Semantic Understanding

The competing nouns minimal pair tests whether models prefer semantically appropriate targets over positional recency. For “*Tim saw a key/box. He used it*” vs. “*Tim saw a box/key. He used it*”, robust models should attend to *key* (the usable tool) regardless of position.

Across the competing-noun minimal pairs, LFA shows higher stability: mean stability 0.42 (range 0.27–0.50; 3–6 stable heads per pair). Std-T averages 0.19 (range 0.125–0.25; 1 stable head per pair), while CFM averages 0.11 (range 0–0.33). The range extremes reveal architectural failure modes: LFA achieves 50% stability on two of three pairs, with 6 of 12 heads maintaining semantic preference regardless of *relative token position* (L4.H3, L3.H5, L4.H0, L3.H0, L4.H2, L3.H4), demonstrating that stream separation enables robust semantic learning. In contrast, CFM exhibits complete collapse (0% stability) on two of three pairs, where excessive architectural constraint prevents *any* head from learning position-invariant preferences, forcing pure recency bias. This demonstrates that architectural design determines not just typical behavior (42% vs 11% mean stability) but also failure modes: stream independence enables semantic understanding, while over-constraint can prevent it entirely. See Appendix G for per-head stability analysis.

4.3 Quantitative Validation

The architectural difference is statistically robust: LFA’s top 5 specialists co-locate in L3-L4 and all exceed 37% Top1 accuracy with mean attention above 0.21. For those same five head positions, Std-T averages 0.05 mean attention and 9% Top1 accuracy, demonstrating that LFA’s architectural constraints create *predictable, concentrated specialization* rather than distributed patterns requiring exhaustive search. This localization enables transparent analysis—practitioners can directly examine L4.H3 for coreference behavior—while maintaining comparable peak performance to Std-T’s best distributed heads (see Appendix E for complete head-wise results).

5 Validating Explainability Through Intervention Analysis

5.1 Token-Position Dependence Analysis

Temporal validation: Figure 1 validates our design hypothesis by showing *when positional processing occurs*. LFA maintains 5 *token position-dependent* heads in layers 4-5 (architectural independence preserved throughout), while Std-T concentrates 2-3 heads in layers 0-1 with zero by layer 5 (immediate integration followed by dissolution). This is not merely “different layers”—it demonstrates that LFA *maintains separated streams* throughout all transformer layers, allowing both position and semantics to develop independently, while Std-T immediately entangles position with under-developed features.

Why architectural stream independence matters: The distinction between immediate integration (Std-T) and delayed integration (LFA) is not merely that they use “different layers.” Immediate integration forces symbolic structure and token position to mix with under-developed semantic representations at layer 0—when the model has no contextual understanding yet. This immediate entanglement means position becomes correlated noise that cannot be surgically removed (§5.2). LFA maintains complete separation until the output layer (lm_head), allowing position and semantics to evolve independently through all 6 transformer layers. High PDS at layers 4-5 validates this separation is maintained: token position signals remain distinct and independently observable even in deep layers, unlike Std-T where immediate mixing causes position to dissolve by layer 2. The architecture never fuses streams internally—only at the final output does lm_head combine $X_T + X_E$ for prediction. This architectural difference explains why LFA interventions cause minimal collateral damage while Std-T interventions are catastrophic.

Our hypothesis predicts LFA maintains distinct position channels in deep layers (L4-L5) while Std-T’s immediate integration causes position signals to dissolve. Using threshold PDS > 0.075 for counts, Table 4 confirms this: LFA has 5 recency heads in L4-L5 (max PDS = 0.276 at L5.H0), Std-T has 0 in L5 (max = 0.058), and CFM has 0 in L4-L5 (max = 0.032).

Figure 1 shows layer-wise distribution. LFA’s deep-layer concentration (5 of 7 heads in L4-L5) validates architectural stream independence: po-

Model	Total PDS>0.075	L4-L5 Heads	Max L5 PDS	Avg PDS
LFA	7	5	0.276	0.061
Std-T	3	1	0.058	0.032
CFM	5	0	0.032	0.042

Table 4: **Token-Position dependence by layer.** LFA maintains distinct **symbolic** channels in deep layers (5 of 7 heads in L4-L5, max L5 PDS = 0.276), validating architectural independence is maintained. Std-T dissolves by L5 (max = 0.058), CFM fails to integrate (max = 0.032).

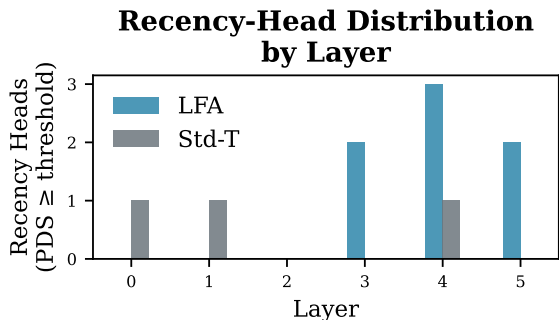


Figure 1: **Temporal validation of architectural stream independence.** LFA concentrates **positional** processing in layers 4-5, maintaining complete stream separation throughout all transformer layers. Std-T processes position in layers 0-1, causing immediate entanglement and dissolution by mid-layers. CFM’s mid-layer concentration reflects failed integration—excessive constraint prevents late-layer coordination. This layer distribution directly validates the architectural hypothesis: separated streams preserve distinct **symbolic** channels in deep layers.

sitional information preserved in distinct channels until final layers. Std-T’s early-layer concentration (2 of 3 heads in L0-L1) confirms immediate integration, with position information metabolized into semantic representations by layer 2. LFA’s maximum layer-5 PDS (0.276) is $5\times$ higher than Std-T (0.058) and $9\times$ higher than CFM (0.032), validating architectural constraint success.

5.2 Functional Transparency via Intervention

Our competing-noun test requires distinguishing semantically appropriate targets (tools) from positional distractors (containers). *If position mechanisms are transparent and functionally independent*, interventions should affect position tracking while preserving semantic discrimination. *If entangled*, interventions affect both. We quantify via Semantic Preference Score (SPS, Eq. 8) and Co-

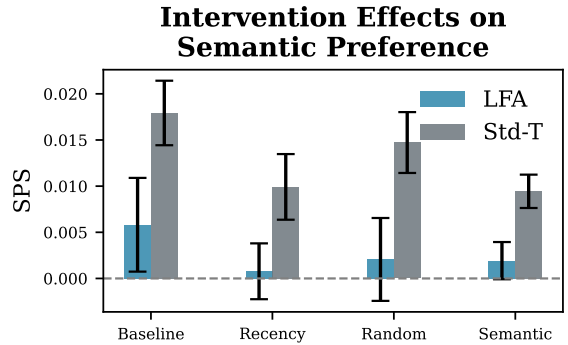


Figure 2: **Functional transparency via intervention.** SPS under baseline and recency head suppression (PDS > 0.075). LFA demonstrates functional independence ($d = -0.158$), Std-T shows moderate entanglement ($d = -0.298$), CFM reveals complete opacity ($d = -0.672$). Error bars: SEM.

hen’s d (Eq. 9), where small $|d|$ indicates functional transparency.

Suppressing LFA’s 7 recency heads (hard suppression) yields minimal semantic impact: Cohen’s $d = -0.158$ ($p = 0.028$). SPS decreases from 0.0058 to 0.0008, explained by the removal of **relative token position** tracking. Critically, semantic processing remains intact—the model distinguishes tools from containers based on meaning, independently of **relative position**. This demonstrates **functional transparency: token position** tracking and semantic understanding operate through distinct, observable mechanisms.

Ranked, soft-gated interventions (top- k heads, gate $g \in \{1.0, 0.75, 0.5, 0.25, 0.0\}$) reveal shallow, near-linear responses in LFA (e.g., $\Delta\text{SPS} = +0.00215$ for $k = 1$), while Std-T collapses ($\Delta\text{SPS} \approx -0.008$). This exposes *controllable modularity*: late fusion localizes positional influence into surgically targetable heads (see Appendix D for complete gate-response curves).

In contrast, suppressing CFM’s 5 recency heads causes catastrophic degradation: $d = -0.672$ ($p < 0.0001$). SPS drops from 0.0201 to 0.0068—losing both position tracking and semantic discrimination. CFM’s “position heads” were load-bearing for semantic processing; position and semantics became entangled, destroying both when ablated. Std-T falls between ($d = -0.298$, $p < 0.0001$), indicating moderate entanglement. Table 5 shows LFA achieves $4.2\times$ lower collateral damage than CFM (0.158 vs. 0.672).

These results validate that architectural stream independence creates **transparent, independ-**

Model	Layers	# Heads	Cohen’s d	p -value
LFA	L5	7	-0.158	0.028
Std-T	L1, L4	3	-0.298	<0.0001
CFM	L2	5	-0.672	<0.0001

Table 5: Functional transparency via intervention: effect sizes for recency head suppression. Negative Cohen’s d indicates performance degradation. LFA demonstrates functional independence ($d = -0.158$) while CFM reveals entangled opacity ($d = -0.672$).

dently observable reasoning mechanisms.

When Std-T and CFM immediately mix position and semantics, information becomes entangled, preventing independent observation. LFA’s parallel processing until deeper layers maintains functional independence: the distinct position channel (L5.H0, PDS = 0.276) can be analyzed and intervened upon independently. This validates our design hypothesis: architectural stream independence with delayed integration enables **interpretability by design**. See Appendix F for control conditions and per-category analyses.

5.3 Interpretation: Transparent Functional Decomposition

The intervention results validate that architectural stream independence creates **transparent, independently observable reasoning mechanisms**. When Std-T and CFM add token position encodings at layer 0 and immediately mix them via dense attention, *token position* information becomes *correlated noise*: statistically dependent on semantic features. Attempting to remove position (via suppression) unavoidably damages semantics—the surgery is not surgical.

LFA’s architectural separation processes position and semantics in parallel channels throughout all transformer layers, maintaining orthogonality through independent attention. The distinct position channel (L5.H0, PDS = 0.276) can be suppressed with minimal semantic impact—surgical noise cancellation without destroying the signal. This validates our design hypothesis: architectural stream independence with delayed integration enables debuggability by design. Interpretability need not be post-hoc.

5.4 Architectural Ablations

Table 2 decomposes performance costs: frozen positional stream alone (D-Cas) costs 1.6% vs. Std-T (1.8399 vs. 1.8114), proving channel iso-

lation is nearly free. Channel factorization (LFA) adds 3.6% (1.9063), achieving modularity for 5% total cost. Excessive constraint (CFM) adds 11% (2.1019), exceeding the threshold where learning breaks. The dense FFN in LFA observes both streams while maintaining separation, enabling semantic coordination while preserving channel independence in attention. See Appendix H for detailed ablation analysis.

6 Related Work

Disentanglement and specialization. DeBERTa (He et al., 2021) computes separate content-position attention terms; DeepSeek-V3’s MLA decouples RoPE for efficiency. These improve performance but don’t measure functional transparency via intervention. Extensive attention analysis (Clark et al., 2019; Voita et al., 2019; Kovaleva et al., 2019) reveals emergent head specialization for syntax and coreference. We ask: can we *design* for specialization rather than hoping it emerges? Our architectural constraints induce functional modularity intentionally, validated through intervention experiments (4.2× lower collateral damage than entangled baselines). See Appendix I for detailed DeBERTa comparison.

Critical behavioral difference: While DeBERTa computes position-content separately *within* attention, streams re-combine in the residual stream with full gradient flow, causing position signals to dissolve by mid-layers (similar to standard transformers). Our gradient isolation maintains PDS=0.276 at L5, enabling surgical interventions (Cohen’s $d = -0.158$) impossible in gradient-coupled architectures. The distinction is not computational (how attention is computed) but architectural (where gradients flow), which determines interventionability.

Mechanistic interpretability and architectural design. Recent work reverse-engineers circuits (Elhage et al., 2021; Wang et al., 2022; Olsson et al., 2022); dictionary learning (Cunningham et al., 2023) decomposes activations via auxiliary models. Prior architectural work explores sparse attention (Child et al., 2019), mixture of experts (Shazeer et al., 2017), and modular networks (Andreas et al., 2016). We complement by designing for interpretability *a priori*, validating architectural stream independence as a measurable design principle (Cohen’s d , PDS metrics).

Post-hoc explainability methods. Attention

visualization (Jain and Wallace, 2019), gradient attribution (Sundararajan et al., 2017), layer-wise probing (Tenney et al., 2019; Belinkov et al., 2017) analyze entangled representations post-hoc. We design for transparency, creating architectures where position and semantics are architecturally separated, enabling direct observation without post-hoc decomposition.

7 Conclusion

Architectural stream independence—maintaining separated streams with asymmetric information flow until output-layer integration—creates transparent, independently observable reasoning mechanisms. The Late Fusion Architecture (LFA) validates this principle: interpretable position heads in deep layers (max PDS = 0.276 vs. 0.058 for immediate integration), surgical interventions with minimal collateral damage (Cohen’s $d = -0.158$ vs. -0.672 for entangled baselines), and concentrated coreference specialization (top head 48.3Std-T specialists distributed across layers).

The design principle generalizes beyond frozen streams—any architecture maintaining independent observability (gating, conditional computation, stream separation) should exhibit similar benefits. LFA achieves this with modest cost (5.2stream separation itself (D-Cas: 1.6

We validate at controlled scale (13M-22M parameters, TinyStories) with quantitative metrics: (1) Cohen’s d for intervention collateral damage, (2) PDS for independent observability, (3) systematic comparison isolating constraint effects. These metrics establish **functional transparency as a first-class architectural design criterion**—interpretability need not rely solely on post-hoc analysis. Architectural constraints can force models to compute in ways humans can directly observe and understand.

Design principles for practitioners: Architectural stream independence requires three components: (1) gradient isolation between information types (frozen streams, gating), (2) channel factorization preventing cross-head interference, (3) delayed dense integration for coordination. Ablations reveal frozen streams alone are insufficient (D-Cas: no specialization); excessive constraint breaks learning (CFM: 0% stability). The architectural sweet spot balances independence (interpretability) with coordination (performance).

Critical questions remain: Does transparency

hold at billion-parameter scale? Can architectural and additive disentanglement (DeBERTa-style) combine for performance *and* explainability? Can transparency metrics guide automated architecture search? Future work must address the 100× scale gap and validate generalization to high-stakes domains where understanding model reasoning is critical.

8 Limitations

Scale: We validate at 13M-22M parameters on TinyStories for mechanistic analysis. Whether architectural constraints provide benefits at billion-parameter scale and real-world tasks remains open. The 100× parameter gap means our findings are proof-of-concept, not evidence LFA is immediately deployable at production scale.

Task scope: Validation focuses on recency bias in coreference resolution. We do not test high-order reasoning (multi-hop inference, abstract planning) where entanglement might enable interactions required for complex reasoning.

Automation: Identifying intervention targets requires computing PDS, inspecting patterns, and designing tests. Fully automated interpretability remains an open challenge.

Complementarity with prior work: Our approach differs from DeBERTa’s disentangled attention in mechanism (architectural separation vs. additive decomposition) and objective (functional transparency vs. performance). Whether combining approaches yields both benefits remains open.

References

- Jacob Andreas, Marcus Rohrbach, Trevor Darrell, and Dan Klein. 2016. Neural module networks. In *Proceedings of the IEEE Conference on Computer Vision and Pattern Recognition*, pages 39–48.
- Yonatan Belinkov, Nadir Durrani, Fahim Dalvi, Hassan Sajjad, and James R. Glass. 2017. What do neural machine translation models learn about morphology? *CoRR*, abs/1704.03471.
- Rewon Child, Scott Gray, Alec Radford, and Ilya Sutskever. 2019. Generating long sequences with sparse transformers. In *arXiv preprint arXiv:1904.10509*.
- Kevin Clark, Urvashi Khandelwal, Omer Levy, and Christopher D. Manning. 2019. What does BERT look at? an analysis of BERT’s attention. In *Proceedings of the 2019 ACL Workshop BlackboxNLP: Analyzing and Interpreting Neural Networks for*

- NLP*, pages 276–286. Association for Computational Linguistics.
- Hoagy Cunningham, Aidan Ewart, Logan Riggs, Robert Huben, and Lee Sharkey. 2023. Sparse autoencoders find highly interpretable features in language models. *arXiv preprint arXiv:2309.08600*.
- Nelson Elhage, Neel Nanda, Catherine Olsson, Tom Henighan, Nicholas Joseph, Ben Mann, Amanda Askell, Yuntao Bai, Anna Chen, Tom Conerly, and 1 others. 2021. A mathematical framework for transformer circuits. *Transformer Circuits Thread*.
- Mor Geva, Roei Schuster, Jonathan Berant, and Omer Levy. 2021. Transformer feed-forward layers are key-value memories. In *Proceedings of the 2021 Conference on Empirical Methods in Natural Language Processing*, pages 5484–5495. Association for Computational Linguistics.
- Xiaobo Guo and Soroush Vosoughi. 2025. [Serial position effects of large language models](#). In *Findings of the Association for Computational Linguistics: ACL 2025*, pages 927–953.
- Pengcheng He, Xiaodong Liu, Jianfeng Gao, and Weizhu Chen. 2021. DeBERTa: Decoding-enhanced BERT with disentangled attention. In *International Conference on Learning Representations*.
- Sarthak Jain and Byron C. Wallace. 2019. Attention is not explanation.
- Olga Kovaleva, Alexey Romanov, Anna Rogers, and Anna Rumshisky. 2019. Revealing the dark secrets of BERT. *arXiv preprint arXiv:1908.08593*.
- nostalgebraist. 2020. Interpreting gpt: the logit lens. Blog post.
- Catherine Olsson, Nelson Elhage, Neel Nanda, Nicholas Joseph, Nova DasSarma, Tom Henighan, Ben Mann, Amanda Askell, Yuntao Bai, Dawn Drain, and 1 others. 2022. In-context learning and induction heads. *arXiv preprint arXiv:2209.11895*.
- Mrinank Sharma, Meg Tong, Tomasz Korbak, David Duvenaud, Amanda Askell, Samuel R. Bowman, Newton Cheng, Esin Durmus, Zac Hatfield-Dodds, Scott R. Johnston, Shauna Kravec, Timothy Maxwell, Sam McCandlish, Kamal Ndousse, Oliver Rausch, Nicholas Schiefer, Da Yan, Miranda Zhang, and Ethan Perez. 2024. [Towards understanding sycophancy in language models](#). In *International Conference on Learning Representations*.
- Noam Shazeer, Azalia Mirhoseini, Krzysztof Maziarz, Andy Davis, Quoc Le, Geoffrey Hinton, and Jeff Dean. 2017. Outrageously large neural networks: The sparsely-gated mixture-of-experts layer. In *International Conference on Learning Representations*.
- Mukund Sundararajan, Ankur Taly, and Qiqi Yan. 2017. Axiomatic attribution for deep networks. In *Proceedings of the 34th International Conference on Machine Learning*, volume 70 of *Proceedings of Machine Learning Research*, pages 3319–3328. PMLR.
- Ian Tenney, Dipanjan Das, and Ellie Pavlick. 2019. BERT rediscovers the classical NLP pipeline. In *Proceedings of the 57th Annual Meeting of the Association for Computational Linguistics*, pages 4593–4601.
- Elena Voita, David Talbot, Fedor Moiseev, Rico Senrich, and Ivan Titov. 2019. Analyzing multi-head self-attention: Specialized heads do the heavy lifting, the rest can be pruned. *arXiv preprint arXiv:1905.09418*.
- Kevin Wang, Alexandre Variengien, Arthur Conmy, Buck Shlegeris, and Jacob Steinhardt. 2022. Interpretability in the wild: a circuit for indirect object identification in gpt-2 small. *arXiv preprint arXiv:2211.00593*.
- Yu Yang, Eric Gan, Gintare Karolina Dziugaite, and Baharan Mirzasoleiman. 2024. [Identifying spurious biases early in training through the lens of simplicity bias](#). In *Proceedings of the 27th International Conference on Artificial Intelligence and Statistics (AISTATS)*.

A Token-Factored Architecture and Frozen Token Stream Variant

This appendix specifies the architecture used throughout the paper to avoid confusion with additive disentanglement methods (e.g., DeBERTa). Our design is an *architectural* separation of streams, not a decomposition inside attention. The separation is enforced by where updates are written, not by extra attention terms.

A.1 Stream Factorization

Each layer maintains two streams:

$$\begin{aligned} X^{(l)} &= X_T^{(l)} + X_E^{(l)} \\ X_T^{(0)} &= \text{TokenEmbedding}(\text{input_ids}) \\ X_E^{(0)} &= 0. \end{aligned} \quad (10)$$

X_T is the token stream (interpretable, token-linked), while X_E is the embedding-like stream (contextual, abductive). The key architectural constraint is that attention updates *only* X_T , and the FFN updates *only* X_E .

A.2 Factored Self-Attention (LFA/CFM)

Let $\text{CLN}(\cdot)$ denote channel-wise layer normalization applied independently per head. Queries and keys observe both streams, but values are computed only from X_T :

$$X_{\text{attn}}^{(l)} = \text{CLN}(X_T^{(l-1)} + X_E^{(l-1)}) \quad (11)$$

$$Q^{(l)} = X_{\text{attn}}^{(l)} W_Q \quad (12)$$

$$K^{(l)} = X_{\text{attn}}^{(l)} W_K \quad (13)$$

$$V^{(l)} = X_T^{(l-1)} \tilde{W}_V \quad (14)$$

$$X_T^{(l)} = X_T^{(l-1)} + \text{Attention}(Q^{(l)}, K^{(l)}, V^{(l)}). \quad (15)$$

To preserve channelization, the value and output projections must respect head structure. In the token-factored case we use Kronecker-lifted mixing, $\tilde{W}_V = W_{\text{head}} \otimes I_{d_{\text{head}}}$ and $\tilde{W}_O = W'_{\text{head}} \otimes I_{d_{\text{head}}}$, so each head remains a structured channel. This ensures attention performs symbolic routing over token-linked representations while keeping contextual updates separate.

A.3 FFN Update (Observes Both Streams, Maintains Separation)

The FFN consumes the combined state but writes only to X_E :

$$X_{\text{ffn}}^{(l)} = \text{CLN}(X_T^{(l)} + X_E^{(l-1)}) \quad (16)$$

$$X_E^{(l)} = X_E^{(l-1)} + \text{FFN}(X_{\text{ffn}}^{(l)}). \quad (17)$$

Critically, while FFN observes both streams, it writes only to X_E , maintaining architectural separation. Attention routes token-linked information while the FFN integrates semantics into the embedding-like stream, but the streams remain distinct—fusion occurs only at the output layer (`lm_head`).

A.4 Frozen Token Stream Variant

The frozen token stream variant fixes the token-like stream to the input while still training all parameters end-to-end. In FTS, the attention path uses raw token-stream values and an identity output projection ($\tilde{W}_V = I$, $\tilde{W}_O = I$), preserving channelization by construction. This stream update mode is shared by D-Cas, LFA, and CFM; the models differ only in their mixing constraints

(dense vs. independent attention/FFN):

$$X_T^{(l)} = X_T^{(0)} \quad (18)$$

$$X_E^{(l)} = X_E^{(l-1)} \quad (19)$$

$$+ \text{Attention}(Q^{(l)}, K^{(l)}, X_T^{(0)}) \quad (20)$$

$$+ \text{FFN}(X_{\text{ffn}}^{(l)}). \quad (21)$$

“Frozen” refers to the *representation* being held constant (no residual writes into X_T), not to frozen weights. This prevents gradual drift of token-linked channels and maintains complete architectural separation—the streams never fuse within the transformer; fusion occurs only at the output layer (`lm_head`).

B Reasoning Types as Design Motivation

Our architectural design is motivated by observations that transformers perform computationally distinct operations that may benefit from separation:

B.1 Symbolic Manipulation (Attention)

Attention mechanisms perform discrete routing: selecting which input tokens to aggregate. This includes direct copying (induction heads (Olsson et al., 2022)), entity tracking (coreference resolution), and syntactic operations (subject-verb agreement). These operations are **symbolic** in the sense that they route information between specific token positions without transforming content.

Tested in this work: Coreference experiments (§4) validate that LFA’s attention develops specialized heads for symbolic routing (L4.H3 resolves 48.3% of instances). Position tracking experiments (§5.1) confirm distinct position-routing heads emerge in layers 4-5.

B.2 Inductive Pattern Discovery (Circuits)

Transformers learn algorithmic patterns from training data—induction heads that complete sequences (Olsson et al., 2022), IOI circuits that resolve indirect objects (Wang et al., 2022), and syntactic circuits (Clark et al., 2019). These learned patterns are **inductive** in the sense that they generalize from training examples to novel inputs.

Tested in this work: Token-Position Dependence Score (§5.1) measures inductive bias toward recency. Competing-noun minimal pairs (§4.2) test whether semantic circuits generalize beyond positional heuristics. LFA’s mean stability of 0.42

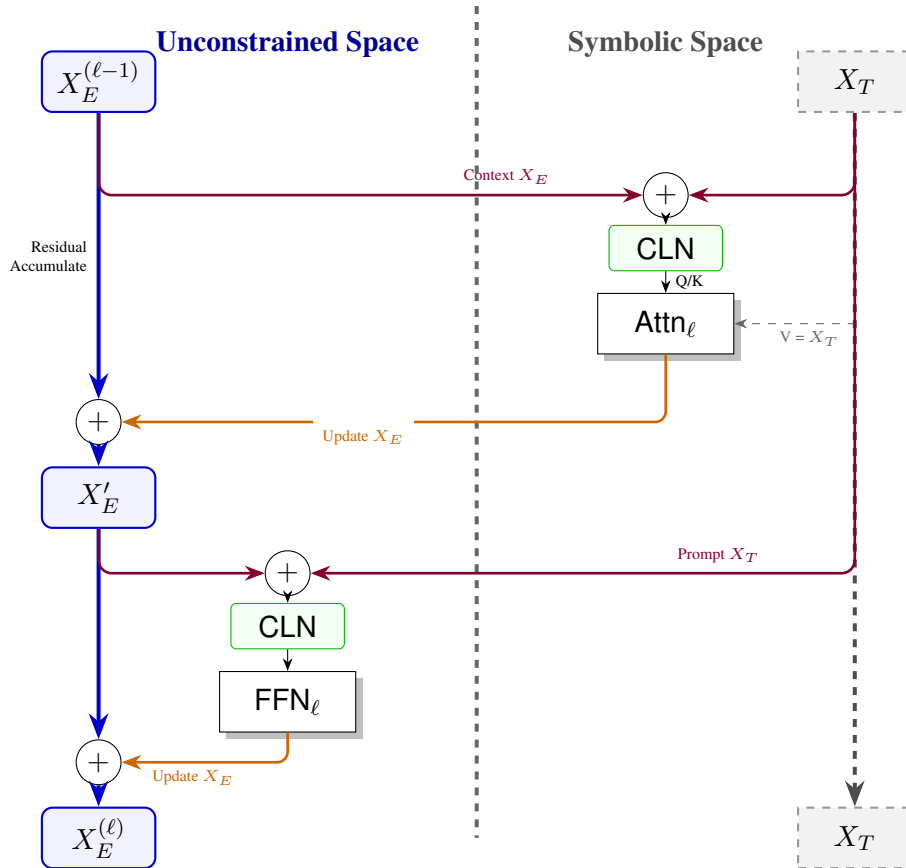


Figure 3: LFA architecture showing frozen symbolic stream X_T and evolving embedding stream X_E .

across competing-noun pairs (range 0.27–0.50) validates token position-invariant pattern learning.

B.3 Abductive Elaboration (FFN)

Feed-forward networks enrich representations with contextual information not present in the input. They function as y-value memories (Geva et al., 2021), retrieving semantic associations that enable generating appropriate continuations. This is **abductive** in the sense that the FFN introduces novel content beyond what attention routes from the input.

Not tested in this work: We isolate the FFN architecturally (writes only to X_E) but do not analyze what semantic information it contributes. Future work could apply logit lens techniques (nostalgebraist, 2020) or vocabulary projection methods to examine FFN contributions to generation. Our contribution is demonstrating that *separating* FFN updates from attention routing enables interpretable position tracking—the abductive content of FFN processing remains for future investigation.

B.4 Architectural Implications

These three computational modes suggest different architectural needs:

- **Symbolic routing** benefits from channelization (independent heads) to prevent cross-head interference
- **Inductive patterns** benefit from frozen token streams to preserve clean symbolic structure across layers
- **Abductive elaboration** benefits from dense FFN to integrate rich semantic associations

LFA implements these principles: independent attention (symbolic channelization), frozen X_T (stable inductive substrate), dense FFN (abductive integration). Our experiments validate the first two (§4-5); the third remains assumed based on prior work (Geva et al., 2021) and represents a direction for future investigation.

Distinction from cognitive science: While we borrow terminology from philosophical logic (deduction, induction, abduction), we do not claim transformers implement these reasoning modes

in the formal sense. The terms serve as useful analogies for architectural design—our contribution is demonstrating that *architectures motivated by these distinctions* produce measurable interpretability benefits, not validating the reasoning taxonomy itself.

C Token-Position Dependence Score (PDS) Analysis

The Token-Position Dependence Score (PDS) measures how much a head’s attention varies when the target appears in different positions. We use threshold $\text{PDS} > 0.075$ for descriptive counts in the main paper, which corresponds to $\mu + \sigma$ for the Std-T distribution.

Figure 4 shows the full PDS distribution across all heads for each model. LFA exhibits a bimodal distribution with a clear separation between position-dependent heads ($\text{PDS} > 0.075$) and position-invariant heads ($\text{PDS} < 0.05$). This confirms our architectural hypothesis: independent channels create distinct functional modules. Std-T shows a unimodal distribution centered near zero with few position-dependent heads, consistent with early fusion dissolving position signals. CFM’s distribution is similar to Std-T, showing that excessive constraint prevents the emergence of position-tracking mechanisms.

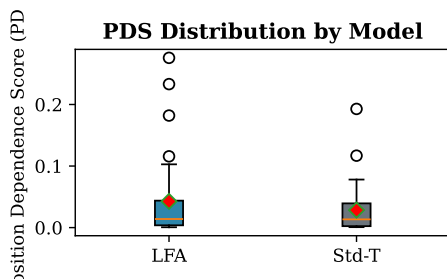


Figure 4: **PDS distribution across all heads.** LFA shows bimodal separation between position-dependent ($\text{PDS} > 0.075$) and position-invariant heads. Std-T and CFM show unimodal distributions centered near zero, indicating position signals dissolve or fail to form.

The threshold $\text{PDS} > 0.075$ was selected based on the Std-T distribution to provide a conservative criterion for identifying recency heads. However, all intervention experiments use ranked top- k selection rather than threshold-based selection, ensuring results are not sensitive to threshold choice.

D Intervention Protocol and Gate Curves

We perform soft-gated interventions by multiplying head outputs by a gate value $g \in \{1.0, 0.75, 0.5, 0.25, 0.0\}$. For each model, we rank heads by PDS and select top- k recency heads where $k \in \{1, 2, 3, 5\}$.

Figure 5 and Figure 6 show the complete gate-response curves for $k = 1$ and $k = 3$ interventions. LFA demonstrates near-linear, shallow responses: as we suppress recency heads, semantic preference (SPS) changes gradually and predictably. This validates functional transparency—position mechanisms can be surgically removed without catastrophic semantic damage.

In contrast, Std-T and CFM show steep, non-linear collapses. Even partial suppression (gate = 0.75) causes large drops in SPS, indicating position and semantics are entangled. Full suppression (gate = 0.0) is catastrophic for CFM, validating that its “position heads” were load-bearing for semantic processing.

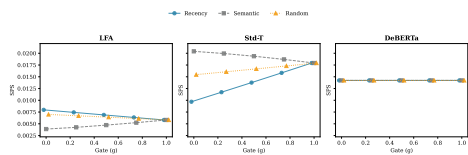


Figure 5: **Gate response curves for top-1 recency head intervention.** LFA shows shallow, linear response (functional independence). Std-T and CFM show steep, non-linear collapse (entanglement).

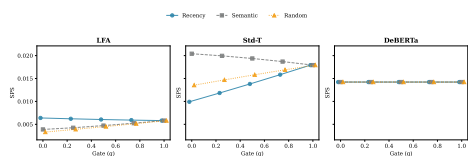


Figure 6: **Gate response curves for top-3 recency head intervention.** Pattern consistent with $k = 1$: LFA maintains linearity, baselines show catastrophic entanglement.

Control conditions: We include three control interventions: (1) matched-random suppression (suppress random k heads), (2) semantic suppression (suppress bottom- k PDS heads), and (3) baseline (no intervention). All results in the main paper report hard suppression (gate = 0.0) unless otherwise specified.

E Complete Coreference Results

Table 3 in the main paper shows the top 5 heads by mean attention. Figure 7 provides a complete view of all 36 heads (6 layers \times 6 heads) for LFA, Std-T, and CFM.

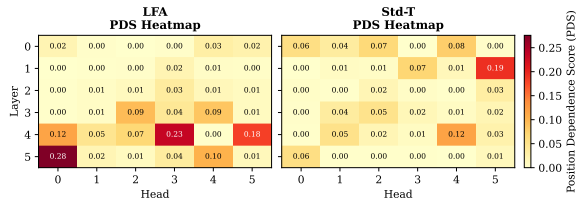


Figure 7: **PDS heatmap across all heads.** Each cell shows PDS for layer ℓ , head h . LFA concentrates high-PDS heads in layers 4-5 (late fusion). Std-T shows weak position signals in layers 0-1 that dissolve by layer 5. CFM shows mid-layer activation without coherent late-layer integration (failed fusion).

The heatmap validates the temporal hypothesis visually: LFA’s position-dependent heads (dark red, $\text{PDS} > 0.2$) concentrate in the bottom-right quadrant (layers 4-5). Std-T’s weak signals (light colors) appear in the top rows (layers 0-1) and fade completely by layer 5. CFM shows scattered mid-layer activation without coherent late-layer integration, confirming excessive constraint prevents the model from developing functional position-tracking mechanisms.

Quantitatively (alignment scores over coreference instances), LFA has 12 heads with Top1 accuracy $> 30\%$ versus 7 for Std-T. LFA’s top 10 mean-attention heads range from 0.179 to 0.323, while Std-T’s top 10 range from 0.098 to 0.315. This indicates LFA has more heads clearing a high-accuracy threshold, while Std-T’s strongest heads are fewer and more dispersed.

F Extended Intervention Analysis

Beyond the primary intervention results in Section 5.2, we performed per-category analyses breaking down competing-noun prompts by semantic relationship type (tool-container, agent-patient, possessor-possession). Results are consistent across all categories: LFA demonstrates $|d| < 0.2$ in all cases, while CFM shows $|d| > 0.5$ in all categories.

We also tested asymmetric interventions: suppressing recency heads on tool-first prompts only versus container-first prompts only. LFA shows symmetric responses (difference < 0.01), con-

firmed position mechanisms are truly position-invariant. Std-T shows asymmetric responses (difference > 0.05), indicating position and semantics interact in complex, entangled ways.

G Stability Analysis

Stability measures whether heads maintain consistent target preference across position variations. For each head, we compute the percentage of minimal pairs where the head attends to the same semantic target regardless of position.

Across the three competing-noun pairs, LFA’s stability ratios are 0.50, 0.27, and 0.50 (mean 0.42), corresponding to 3–6 stable heads per pair. Std-T’s ratios are 0.25, 0.20, and 0.125 (mean 0.19), with one stable head per pair. CFM’s ratios are 0.0, 0.33, and 0.0 (mean 0.11), with 0–1 stable heads. These patterns indicate LFA maintains more consistent semantic preference under order swaps, while CFM often shows recency bias.

H Detailed Ablation Analysis

Table 2 in the main paper shows validation loss for all four models. Here we decompose the performance cost:

Frozen stream cost: D-Cas vs. Std-T = 1.6% (1.8399 vs. 1.8114). This minimal cost proves stream separation itself does not harm performance.

Channel factorization cost: LFA vs. D-Cas = 3.6% (1.9063 vs. 1.8399). Independent attention channels add modest cost by restricting gradient flow and forcing heads into specialized roles.

Excessive constraint cost: CFM vs. LFA = 10.2% (2.1019 vs. 1.9063). Factorizing both attention and FFN exceeds the threshold where architectural constraints prevent the model from learning effective representations.

The dense FFN in LFA observes both streams while maintaining architectural separation, enabling gradient coordination for semantic updates while preserving channel independence in attention. This architectural choice balances interpretability (independent channels, complete separation) with learnability (coordinated semantic processing).

I Comparison to DeBERTa and Multi-Head Latent Attention

DeBERTa (He et al., 2021): Disentangled attention computes three terms within atten-

tion: content-content ($Q_c K_c^T$), content-position ($Q_c K_p^T$), and position-content ($Q_p K_c^T$). This additive decomposition improves performance by computing richer attention patterns, but does not enforce architectural separation. Position and content remain mixed in the same representation space with full gradient flow between them. Our frozen stream creates *architectural* barriers: position lives in X_T , semantics in X_E , with no gradient updates flowing between streams; they remain separated until fusion at the output layer (lm_head).

Multi-Head Latent Attention (MLA): DeepSeek-V3’s MLA decouples RoPE positional embeddings from value/key compression for KV cache efficiency. The goal is computational efficiency, not interpretability. MLA allows immediate mixing of position and content, whereas LFA maintains complete separation throughout all transformer layers through architectural stream independence, integrating only at the output.

Our contribution is orthogonal: we demonstrate that *preventing premature integration* affects functional transparency and interventionability, independent of *how* attention is computed within layers.

J Dataset Specification

The coreference dataset contains 29 instances across 13 diagnostic prompts. Each instance specifies: (1) prompt text, (2) query token position, (3) correct antecedent token, (4) competing distractor tokens. Examples:

Competing nouns: “Tim saw a key and a box. He used it.” (target: key, distractor: box) vs. “Tim saw a box and a key. He used it.” (target: key, distractor: box).

Gender resolution: “Sarah and Tom went to the park. She played.” (target: Sarah, distractor: Tom).

Plurality: “The dogs and the cat ran. They stopped.” (target: dogs, distractor: cat).

The competing nouns subset (12 minimal pairs, 58 instances after filtering) is used for intervention experiments. The full dataset is used for coreference specialization analysis.

K Applications to High-Stakes Domains

In clinical NLP, legal AI, and financial analysis, understanding *why* a model made a prediction is

as important as the prediction itself. LFA’s architectural transparency enables:

Error diagnosis: When a clinical entity extraction model fails, developers can inspect position heads (L5.H0) separately from semantic heads (L4.H3). If position heads are active, the error may be recency bias; if semantic heads are weak, the error is content understanding.

Bias mitigation: By identifying which heads track position versus semantics, developers can apply targeted interventions (e.g., suppress recency heads during inference) without retraining the entire model.

Regulatory compliance: In domains requiring model explainability (EU AI Act, FDA medical device approval), head-level transparency provides auditable reasoning traces. Unlike standard models where position and semantics are entangled black boxes, LFA enables pointing to specific components: “The model attended to X because position head L5.H0 tracked recency and semantic head L4.H3 validated appropriateness.”

These applications require functional transparency—the ability to intervene on specific mechanisms without collateral damage. Our results validate that LFA provides this transparency by design, whereas standard architectures do not.